Original Article

ELSEVIER

nanomedicine
Nanotechnology, Biology, and Medicine

Chitosan polyplex mediated delivery of miRNA-124 reduces activation of microglial cells in vitro and in rat models of spinal cord injury

Andrew M. Louw, PhD[a], Mallappa K. Kolar, MD[b], Liudmila N. Novikova, PhD[b], Paul J. Kingham, PhD[b], Mikael Wiberg, MD, PhD[b], Jørgen Kjems, PhD[a,*], Lev N. Novikov, MD, PhD[b,*]

[a]Interdisciplinary Nanoscience Center, Aarhus University, Aarhus C., Denmark
[b]Department of Integrative Medical Biology, Umeå University, Umeå, Sweden

Abstract

Traumatic injury to the central nervous system (CNS) is further complicated by an increase in secondary neuronal damage imposed by activated microglia/macrophages. MicroRNA-124 (miR-124) is responsible for mouse monocyte quiescence and reduction of their inflammatory cytokine production. We describe the formulation and *ex vivo* transfection of chitosan/miR-124 polyplex particles into rat microglia and the resulting reduction of reactive oxygen species (ROS) and TNF-α and lower expression of MHC-II. Upon microinjection into uninjured rat spinal cords, particles formed with Cy3-labeled control sequence RNA, were specifically internalized by OX42 positive macrophages and microglia cells. Alternatively particles injected in the peritoneum were transported by macrophages to the site of spinal cord injury 72h post injection. Microinjections of chitosan/miR-124 particles significantly reduced the number of ED-1 positive macrophages in the injured spinal cord. Taken together, these data present a potential treatment technique to reduce inflammation for a multitude of CNS neurodegenerative conditions.

From the Clinical Editor: The treatment of spinal cord injury remains an unresolved problem. Secondary damage is often the result of inflammation caused by activated microglia and/or macrophages. In this article, the authors developed their formulation of chitosan/miR-124 polyplex particles and investigated their use in the suppression of neuronal inflammation. This exciting data may provide a new horizon for patients who suffer from spinal cord injury.

Estimations of the annual incidence of patients surviving spinal cord injury (SCI) are approximated at 40 cases/million people, and in the United States alone, 240-337,000 people are currently living with a SCI.[1] Regeneration of injuries in the CNS are hampered by a number of inhibitory proteins and the glial scar - a physical obstruction made up of extracellular matrix created by fibroblasts and hypertrophic astrocytes which respond to stimuli produced by activated microglia/macrophages.[2]

During development, microglia arise from hematopoietic stem cells, common myeloid progenitors, and erythromyeloid precursors, at which point they spatially and functionally separate from their mononuclear phagocyte relatives.[3,4] Macrophages are the effector cells in the inflammatory response at CNS lesions and are derived from microglia and hematogenous monocytes, which are functionally indistinguishable by their morphology and antigenic markers. Therefore, in the context of CNS injury, activated microglia are referred to as macrophages/microglia.

Activated macrophages/microglia are a chronic source of many cytotoxic substances, such as the pro-inflammatory cytokine, tumor necrosis factor alpha (TNF-α),[5] inducible nitric oxide synthase (iNOS),[6] hypochlorous acid,[7] and reactive oxygen species (ROS).[8] After the initial insult, secondary inflammation occurs, which leads to enhanced damage to the tissue in the form of neurodegeneration and impaired regeneration. Indeed, several studies involving anti-inflammatory treatment after trauma, implicate classically activated (M1 polarized) macrophages/microglia as instigators of secondary

tissue damage.[9–11] Activated macrophages/microglia also secrete large amounts of matrix metalloproteases (MMPs), which contribute to degradation of the vascular basement membrane, leading to increased permeability for infiltrating inflammatory cells.[12] Reactive microgliosis after SCI is a condition that describes the self-perpetuating cycle of initial neuron damage, myelin debris activating microglia, which in turn up-regulates pro-inflammatory cytokines and neurotoxic molecules, thereby causing more tissue damage and continuing the cycle of activation/disruption.[13–15] Therefore, similar to other neurodegenerative diseases, SCIs are progressive conditions caused by an increase in secondary neuronal damage due to chronic activation of microglia/macrophages. While it is environmentally favorable for M1 macrophages to maintain an active state by TNF-α positive feedback, they do maintain plasticity if their cytokine environment changes.[16] There is currently no effective treatment for SCI, but modulation of macrophage state of activation could have a positive effect by reducing the secondary tissue damage.

Unraveling the roles of micro-RNA (miRNA) in cells has given us more insight into the phenotypic regulation of cells during development and disease states. Similar to small interfering RNA (siRNA), miRNAs are ~23nt long endogenous ribonucleic acid species that specifically pair with target mRNAs post-transcriptionally to direct mRNA degradation machinery and repress protein translation.[17] miRNA-124, known as the most abundant miRNA found in neurons, is associated with promoting neuronal differentiation in neural progenitor cells.[18,19] It has also been shown to mediate microglia quiescence by controlling two central transcription factors, CCAAT/enhancer binding protein-alpha (C/EBP-alpha) and its downstream target PU.1.[20] These factors are involved in the developmental regulation of non-myeloid cells, specifically, the fibroblast – macrophage transition.[21,22] miRNA-124 has multiple target sites in the 5′ and 3′ UTR of C/EBP-alpha and it was subsequently discovered that miRNA-124 is highly expressed in resident microglia while being down regulated in inflamed tissue.[20,23] As such, the administration of miR-124 to monocytes is associated with decreased levels of TNF-α, and iNOS.[20,24] It has been shown that miR-124 specifically regulates TNF-α production via its targeting of signal transducer and activator of transcription 3 (STAT3), which in turn decreases production of TNF-α converting enzyme (TACE).[25]

Delivery of naked miRNA mimics (in the form of a siRNA) to tissues is hampered by endogenous RNase degradation and poor transfection efficiency/uptake into cells. There are many solutions available for researchers to introduce RNAi into cells, but the majority of commercial reagents are not cell type-specific. As such, there is a need for the targeted delivery of RNAi to cells and tissues to affect disease states without interfering with gene expression in other cells. A simple system, which has some level of cell selectivity, is the chitosan polyplex carrier system.

Chitosan is a linear disaccharide made of D-glucosamine and N-acetyl-D-glucosamine and is derived from the de-acetylation of the naturally abundant chitin found in crustacean exoskeletons. As chitosan is a positively charged molecule of varying sizes, it conveniently interacts with negatively charged double stranded RNA to form polyplexes.[26] The ratios of the two components (the N/P ratio) can be varied to control surface charge and size of the particles.[26,27] Chitosan/siRNA particles have been extensively employed as a non-toxic siRNA delivery vehicle to a number of cell types.[26,28–31] However, a transfection preference for mononuclear phagocytes has been demonstrated for murine peritoneal macrophages in models of radiation induced fibrosis and arthritis.[29,31]

In the present study we employ the chitosan/siRNA polyplex system to introduce a miRNA-124 mimic into rat microglia *ex vivo* and *in vivo* using a model for traumatic spinal cord injury with the goal of reducing/preventing the inflammatory effects and secondary neuron damage induced by the activated microglia/macrophage secretome in the spinal cord. Due to the intrinsically invasive nature of local injections, an intraperitoneal administration of particles to a rat spinal hemisection model is also assessed.

Methods

Preparation of chitosan polyplex particles

All chitosan (250 kDa, 150 kDa and 30 kDa) was purchased as 95% de-acetylated from Heppe Medical Chitosan GMbH (Frankfurt, Germany) and used to prepare polyplexes as described previously.[32] Briefly, chitosan is dissolved in acetate buffer (300 mM, pH 5.5) overnight and filtered through a 0.2 μm syringe filter to obtain a 1 mg ml^{-1} solution. To create particles, Cy3™ dye-labeled siRNA specific to enhanced green fluorescent protein (sense 5′-GACGUAAACGGCCACAAGUUC-3′, and antisense, 3′-CGCUGCAUUUGCCGGUGUUCA-5′), miRNA precursor negative control #1 (AM17129, Life Technologies) or pre-miR™ miRNA precursor, miR-124 (AM17100, life technologies) were each diluted in acetate buffer, and chitosan solution was added to the calculated N:P (N:P 50) molar ratio while stirring for 1 h at room temperature. Particles formulated using eGFP siRNA-Cy3, AM17129 and AM17100, are hereafter referred to as siRNA-Cy3, miR-CTRL, and miR-124, respectively. Chitosan particle formulations were analyzed for their hydrodynamic diameter by photon correlation spectroscopy, and zeta potential by laser doppler velocimetry (LDV) using a Zetasizer Nano ZS (Melvern Instruments, Malvern, U.K.).

Ex vivo experiments

Neonatal rat microglia isolation

Microglia were isolated with modifications to existing methods by mechanically homogenizing the CNS tissue of neonatal rats.[33,34] Briefly, neonatal P4-5 Wistar Hannover rats were sacrificed by exposure to CO_2 and decapitated. Brains and spinal cords where extracted using standard techniques and placed in phosphate buffered saline with 0.2 % glucose (PBSg). The meninges were removed using a micro-dissection microscope and microsurgical forceps. The CNS tissue was cut into pieces and homogenized using a 15 ml wheaton® dounce tissue homogenizer along with 5 ml of PBSg per brain/spinal cord. The homogenate was filtered with a 40 μm falcon cell strainer

(Thermo Fisher Scientific) and suspended in 1.085 g cm^{-2} Percoll® (Sigma-Aldrich, St. Louis, USA) in PBSg and overlaid with 1.045 g cm^{-2} Percoll® in PBSg. After centrifugation at $1250 \times g$ for 45 min with minimum brake and acceleration in a swinging bucket rotor, the purified microglia are located at the Percoll® gradient's interface. Microglia were washed of Percoll® and suspended in growth medium composed of DMEM (Gibco, Life Technologies) supplemented with 10% performance plus endotoxin free, certified fetal bovine serum (Gibco, Life Technologies) with penicillin/streptomycin (Gibco, Life Technologies) and plated as required. Isolated cell purity was assessed by flow cytometric analysis. For flow cytometry experiments, microglia were seeded at a density of 0.5×10^5 per well in 6 well plates. To activate the microglia, cultures were treated with 20 ng ml^{-1} interferon gamma (IFN-γ), and 100 ng ml^{-1} lipopolysaccharide (LPS) and for 1 h and 24 h, respectively, after which the cells were washed and the media replaced daily.

Polyplex cytotoxicity assay

Microglia were seeded in a 96-well plate at a density of 5×10^4 cells per well in 100 µl growth medium. AlamarBlue® (Life Technologies) was used according to the manufacturer's guidelines to assess viability of microglia after a 48 h treatment with Chitosan/miRNA particles. Absorbance was measured at 570 nm using a FLUOstar OPTIMA (BMG Labtech, Offenburg, Germany).

Polyplex uptake studies

Isolated primary microglia were plated at 5×10^4 cells/well in 8 well chamber slides™ (Sigma-Aldrich, Cat# C7182) for 48 h and transfected with chitosan/Cy-3 particles for 2 h. Cells were washed in cold PBS with 1% sodium azide, stained using wheat germ agglutinin Alexa Fluor® 488 (WGA-A488) conjugate (Life Technologies) as per manufacturer's instructions and fixed in 4% paraformaldehyde (Electron Microscopy Sciences). Coverslips were mounted using Prolong Gold® with DAPI (Life Technologies), and slides were imaged with a LSM 700 confocal laser scanning microscope (Zeiss, Germany) using the 63×/1.4 oil objective with 8-bit depth. Fluorescence signals were captured within the dynamic range of the signal intensity and background was corrected by ImageJ (http://rsbweb.nih.gov/ij/, National Institutes of Health, USA).

Microglia supernatant assays

Microglia were isolated and expanded in 6 well plates in growth media with added 5 ng ml^{-1} granulocyte macrophage colony stimulating factor (GM-CSF) (R&D Systems, Minneapolis, MN, U.S.A.). Cells were activated using IFN-γ and LPS and treated with particles for 2 h; termination of the experiment occurred 48 h post-transfection. All supernatants were collected during media changes each day and frozen at -80 °C for analysis. A Greiss® reagent kit (Molecular Probes) for nitrite species quantification was used according to manufacturer's instructions. Absorbance was quantified at 540 nm using a FLUOstar OPTIMA plate reader (BMG Labtech). Secreted TNF-α was quantified using an enzyme linked immunosorbent assay (ELISA) kit (Life Technologies) according to the manufacturer's instructions, and quantified by measuring absorbance at 485 nm using a FLUOstar OPTIMA plate reader (BMG Labtech).

Flow cytometry

Cells were washed twice before harvesting by gentle scraping and pelleted by centrifugation. Microglia were suspended at a concentration of 0.5×10^6 cells per sample and blocked for 10 min using 5% mouse serum in flow buffer (FB) (PBS containing 0.5% bovine serum albumin, and 1% sodium azide). Blocking medium was removed and the cells were immuno-labeled at 4 °C for 45 min in 100 µl FB containing antibodies. Mouse anti-rat antibodies, PE anti-rat RT1B (OX6) and Alexa Fluor® 488 anti-rat CD11b (Ox-42) were purchased from Biolegend, San Diego, CA, USA and titrated to determine appropriate final concentrations. After incubation, cells were washed three times and suspended in 500 µl flow buffer and analyzed on a Gallios™ flow cytometer (Becton Dickenson, San Jose, CA). Single cell analysis was assured by gating the dominant population from forward scatter time of flight versus forward scatter peak. This population was subsequently gated for morphology using standard techniques. Quadrant gating for fluorescent channels was performed using standard fluorescence minus one (FMO) control techniques. Fluorescent cytometric data was analyzed using Kaluza software (Becton Dickenson, San Jose, CA).

In vivo experiments

Experimental animals

The experiments were performed on adult (16 weeks old, n = 32) female Sprague-Dawley rats (Charles River Laboratories, Germany). The animal care and experimental procedures were carried out in accordance with Directive 2010/63/EU of the European Parliament and of the Council on the protection of animals used for scientific purposes, and were also approved by the Northern Swedish Committee for Ethics in Animal Experiments (No. A36-12). All surgical procedures were performed under general anaesthesia using a mixture of ketamine (Ketalar, Parke-Davis; 100 mg/kg i.v.) and xylazine (Rompun®, Bayer; 10mg/kg i.v.). After surgery, the rats were given the analgesic, Finadyne (Schering-Plough, Denmark; 2.5 mg/kg, s.c.), normal saline (4 ml, s.c.) and benzylpenicillin (Boehringer Ingelheim; 60 mg, i.m.). Each animal was housed alone in a cage after surgery and exposed to 12 h light/dark cycles, with free access to food and water.

Injection of polyplex particles

For injections of particles into the normal spinal cord, cervical C3-C4 laminectomy was performed and rats were mounted in a stereotaxic frame (Stoelting's Lab Standard Stereotaxic Instrument, Stoelting Co., USA). A glass micropipette (outer tip diameter 70 µm) was attached to a 5 µl Hamilton syringe, filled with 35 ng µl^{-1} miRNA particles suspended in acetate buffer pH 5.5, and 1 µl of particles was slowly (10 minutes) pressure-injected into the lateral funiculus (depths 1.0 mm) in 3 sites along the rostro-caudal axis of the C3-C4 spinal segments at approximately 1 mm from each other. The micropipette was left in place for additional 2–3 min. Dura mater was covered with Spongostan®, muscles and skin were closed in layers.

For injections of particles in animals with spinal cord injury, the C3 spinal cord segment was exposed and transected on the left side with fine scissors under an operating microscope. The lesion included the lateral funiculus as well as the adjacent grey
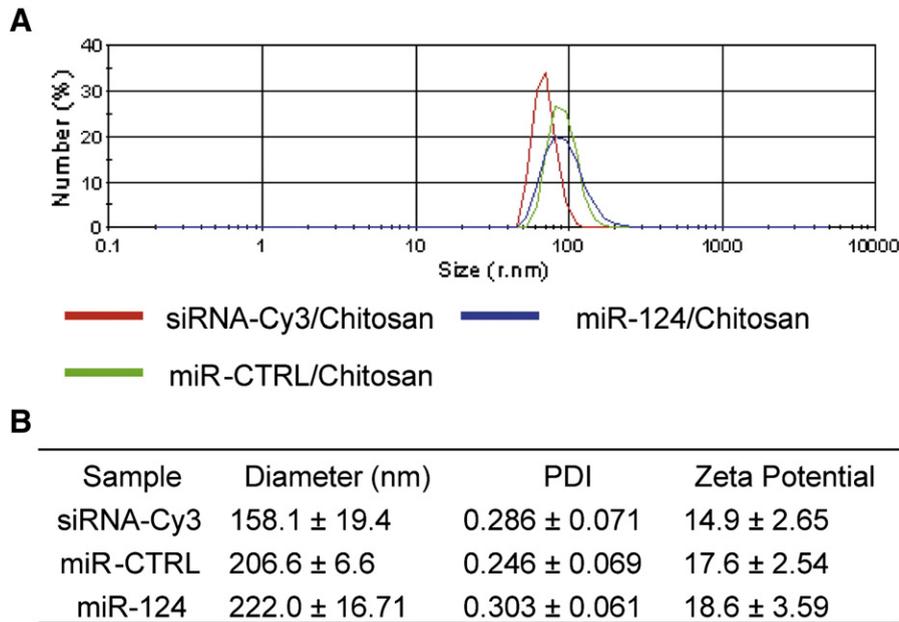
Figure 1. Chitosan particle characterization by photon correlation spectroscopy and laser Doppler velocimetry (LDV). Representative histograms of particle radius and dispersity (**A**). The size (diameter in nm), polydispersity index (PDI) and zeta potential of the particles (**B**).

matter. Particles were pressure-injected into the lateral funiculus (depths 1.0 mm) at approximately 1 mm rostral and 1 mm caudal to the lesion site as described above. For intraperitoneal injections, 1 ml solution of particles labelled with Cy-3 was used.

In a separate group of animals, the trauma zone was expanded in the rostro-caudal direction by gentle aspiration to create a 1–2 mm long cavity in the C3 spinal segment. A small piece of Spongostan® was soaked in 1 μl of 35 ng μl^{-1} miRNA particles suspended in acetate buffer pH 5.5 and implanted into the cavity. The injury site was covered with fibrin glue (Tisseel® Baxter SA, Switzerland) and muscles and skin were closed in layers.

Tissue processing

At 3 h, 24 h, 2 days, 3 days and 7 days, the animals were deeply anaesthetized with an intraperitoneal overdose of sodium pentobarbital and transcardially perfused with Tyrode's solution followed by 4% paraformaldehyde in 0.1 M phosphate buffer (pH 7.4). Spinal cord segments C2–C5 were removed and transferred into the same fixative for 3–4 h. Tissue blocks were then cryoprotected in 10% and 20% sucrose for 2–3 days and frozen in liquid isopentane. Serial longitudinal 16-μm-thick sections were cut on a cryomicrotome (Leica Instruments, Germany), thaw-mounted in pairs onto SuperFrost™ Plus slides, dried overnight at room temperature and stored at −85 °C before processing.

Immunohistochemistry

After blocking with normal serum, the following primary antibodies were used: rabbit anti-GFAP (1:1000; Dako), mouse anti-ED-1 (1:100, Abcam), mouse anti-OX-42 (1:250; Serotec), mouse anti-NeuN (1:200; Chemicon). All primary antibodies were applied for 2 h at room temperature. After rinsing in PBS, secondary goat anti-mouse and goat anti-rabbit antibodies Alexa

Fluor® 488 and Alexa Fluor® 568 (1:300; Molecular Probes, Invitrogen) were applied for 1 h at room temperature in the dark. The slides were mounted with ProLong® mounting media containing DAPI (Invitrogen). The staining specificity was tested by omission of primary antibodies.

Quantification of macrophage/microglial reaction

Reaction of ED1-positive macrophages and microglial cells was studied in the spinal cord trauma zone in 20 randomly selected sections after injection of particles containing miR-NA-CTRL or microRNA-124. The images were captured at 400 final magnifications and 1280×1024 pixels resolution with a Nikon DS-U2 digital camera, imported into Image-Pro Plus software (Media Cybernetics, Inc, USA) and the relative tissue area occupied by labelled profiles was quantified.

Statistical analysis

One-way analysis of variance (ANOVA) followed by a post hoc Newman-Keuls Multiple Comparison Test and unpaired t-test were used to determine statistical differences between the experimental groups (Prism®, GraphPad Software, Inc, USA).

Results

Characterization of chitosan polyplex particles

Chitosan particles formulated at N:P ratio 50 with either miR-124 mimic (miR-124), a scrambled miRNA control mimic (miR-CTRL), or a Cy3 labeled unrelated siRNA (siRNA-Cy3) were evaluated for size, polydispersity and zeta potential (Figure 1). The size of the particles formulated with the miRNA precursors were similar to each other: 206.6 ± 6.6 nm for miR-CTRL and 222.0 ± 16.71 nm for miR-124 while the
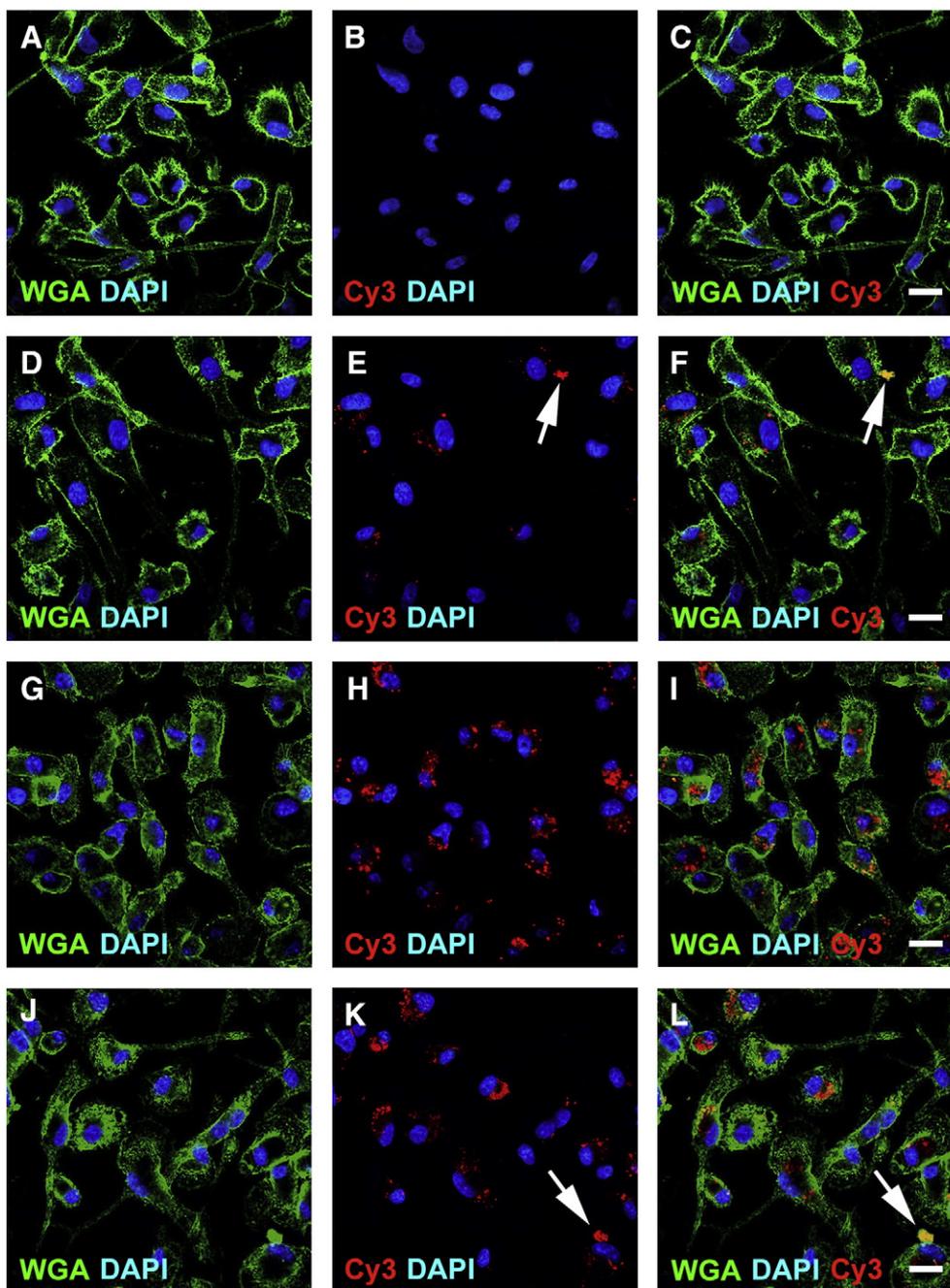
Figure 2. Representative confocal scanning laser microscopy images of untreated primary rat microglia (**A–C**) labelled with wheat germ agglutinin Alexa Fluor® 488 conjugate (WGA, green) and DAPI (blue), and images showing intracellular uptake of chitosan particles containing 5 μM (**D–F**), 25 μM (**G–I**), 50 μM (**J–L**) of siRNA-Cy3 (red) after 2 h treatment. Arrows indicate examples of external chitosan agglomerates. Scale bar, 20 μm.

siRNA-Cy3 resulted in polyplex particles of a slightly smaller size (158.1 ± 19.4 nm; Figure 1, *A*). The polydispersity index showed a narrow distribution of particle sizes for miR-Cy3, miR-CTRL, and miR-124 (0.286 ± 0.071, 0.246 ± 0.069, and 0.303 ± 0.061, respectively). The zeta potential of the particles formulated with the miRNA precursors were similar 17.6–18.6 whereas the siRNA-Cy3 loaded particles was slightly lower most likely due to the added contribution of negative charges from the two sulfonate groups on Cy3 (Figure 1, *B*).

Uptake of particles in primary microglia

siRNA-Cy3/chitosan complexes, formed with variable N:P ratios and molecular weights of chitosan (30, 150, and 250 kDa) were screened for their uptake into primary microglia (data not shown). Of these, a complex formed with 150 kDa chitosan at N:P ratio of 50 was determined to be optimal for transfecting activated primary microglia. Representative fluorescent images of siRNA-Cy3/chitosan particle uptake after 2 hours can be seen
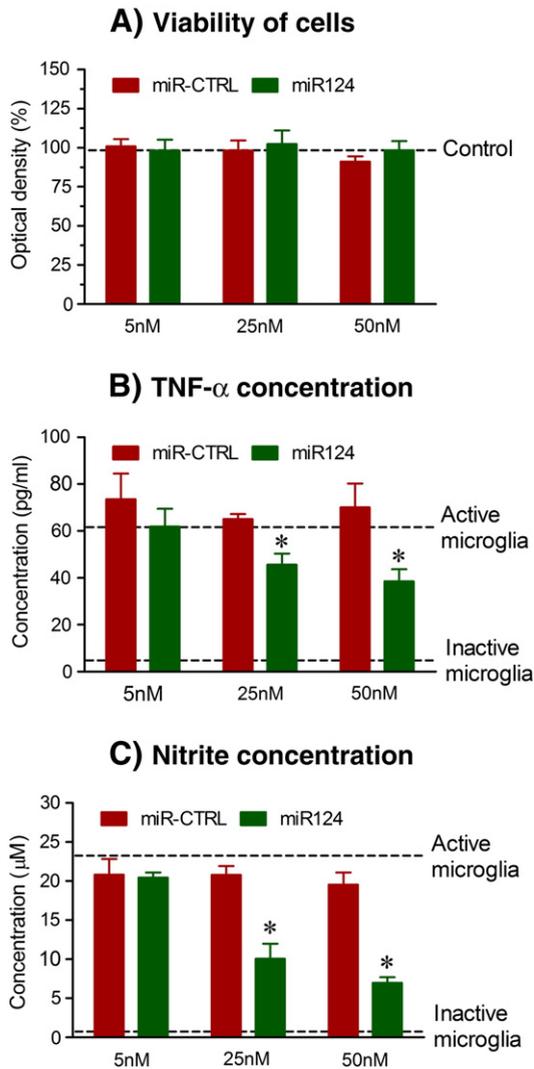
A) Viability of cells

B) TNF-α concentration

C) Nitrite concentration

Figure 3. Isolated microglia were expanded with GM-CSF, activated using LPS and IFN-γ, and treated with miR/chitosan particles. Cells were incubated with particles for 48 h with three different miRNA concentrations. Cytotoxicity of chitosan/miRNA particles measured by AlamarBlue® viability assay **(A)**. Percent viability is expressed relative to untreated controls ± SD (n=3). Activated microglia supernatant assays **(B, C)**. Total supernatant was harvested each day for analysis by TNF-α ELISA **(B)** and Greiss nitrite assay **(C)**. Results indicate concentrations 48 h after particle treatment. ** and *$P < 0.01$ and 0.05 versus LPS and IFN-γ alone (n=3).

in Figure 2. Cell membranes and extracellular chitosan particles were stained using WGA-A488 and internalization of increasing concentrations of chitosan/siRNA-Cy3 can be seen in the merged images. The advantage of using WGA-fluorescent conjugates to visualize cell membranes is multifarious because it binds to n-acetyl-d-glucosamine which is a monomeric unit of chitosan. Therefore, by ensuring that the cell membrane stays impermeable to the WGA-A488 (by fixing the sample after staining), the overlaid image can indicate internal (red Cy3 fluorescence) vs. external (co-localized green and red fluorescence (yellow)) chitosan particles in the merged images (Figure 2, arrows). This was subsequently confirmed by CLSM z-stack images (Supplemental Figure 1).

The toxicity of the particle treatment was evaluated after 48 h incubation by AlamarBlue® staining. Notably, the primary microglia showed no significant decrease in viability after treatment with chitosan particles (Figure 3, *A*).

Polyplex particles mediated reduction of inflammatory factors

Next we investigated the effect of particle treatment on production of TNF- α and nitrite species. Secreted TNF-α was quantified by ELISA and the inducible nitric oxide synthase (iNOS) activity was assessed by measuring nitrite concentration in the cell culture media. When activated with IFN-γ and LPS, microglia secreted an increased amount of TNF-α and nitrite compared to inactive controls, 126.4 ± 11.6 pg ml^{-1} versus 4.9 ± 3.6 pg ml^{-1} and 22.9 ± 2.3 μM versus 0.75 ± 0.6 μM, respectively (Figures 3, *B* and *C*). Upon transfection with 5, 25 and 50 nM of chitosan/miR-124 particles, the increase in TNF-α secretion was reduced 16.4%, 30.7% ($P<0.01$) and 45% ($P<0.01$), respectively, compared to miR-CTRL particles (Figure 3, *B*). Concurrently, transfection with 25 nM or 50 nM miR-124 particles, reduced the production of nitrite by activated microglia by 51.6% and 64%, respectively ($P<0.01$, Figure 3, *C*).

Flow cytometry of microglia

Expanded primary microglia were activated and treated with 50 nM miRNA containing chitosan particles. Prior to the treatment microglia culture purity was >96% estimated by the microglial marker CD11b. Activated (IFN-γ and LPS) cultures were ~94% MHC-II positive and only ~1% of cells were MHC-II positive in normal (inactive) cultures (Figure 4). After 48 h treatment with particles containing miR-CTRL, 90% of the cells showed little change compared to activated controls. Treatment with chitosan/miR-124 particles resulted in ~50% fewer MHC-II positive cells, compared to miR-CTRL particles. Expression of CD11b stayed constant for all samples. This data shows that transfection of miRNA-124 particles with concurrent M1 induction was able to maintain low MHC-II expression in the culture, thereby reducing the number of M1 activated cells in the presence of strong polarizing factors.

Polyplex particle application in spinal cord injury model

Three to seventy-two hours after microinjections of chitosan formulated siRNA-Cy3 particles into C3-C4 segments of normal spinal cord, the Cy3 signal could be detected at the injection sites (Figure 5, *A, D, G*) in the form of small bright round spots (see insertion in Figure 5, *A*) and as a diffuse staining of the surrounding spinal cord parenchyma. The siRNA-Cy3 signal, appears to increase within the first 48 h (data not shown), this may be due to scavenging activity of activated macrophages and microglial cells concentrating the particles in endosomes.

Additional immunostaining with antibodies against glial and neuronal markers (Figure 5, *B, E, H*) revealed that OX42 positive macrophages and microglial cells have a preference to internalize the particles (Figure 5, *B, C*). In contrast, the GFAP positive processes of astrocytes (Figure 5, *E, F*) and NeuN positive neuronal cell bodies (Figure 5, *H, I*) did not show any co-localisation with Cy3.
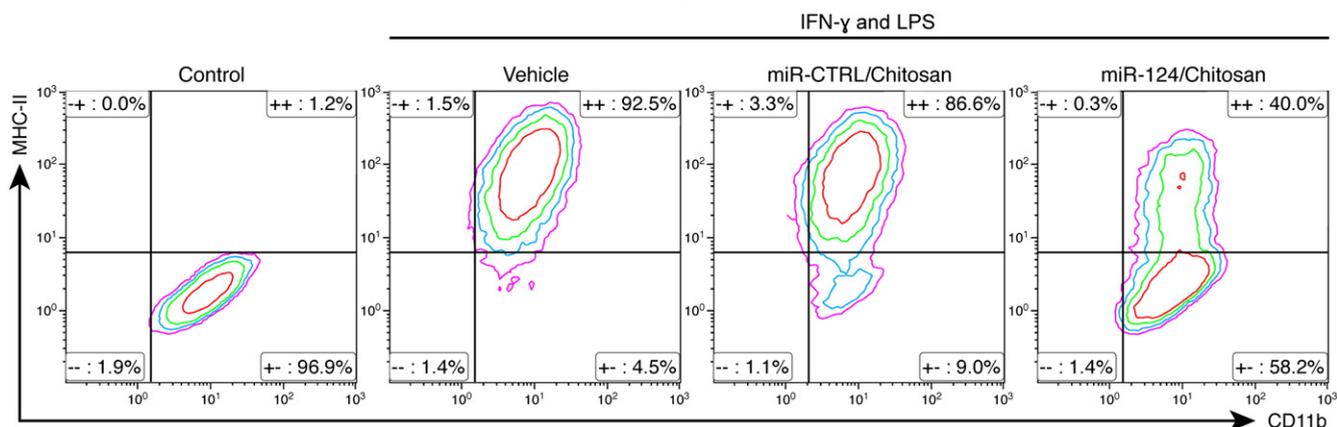
Figure 4. Flow cytometry analysis of MHC-II (y-axis) and CD11b (x-axis) expression in non-activated (Control), activated (Vehicle), and activated microglia treated with chitosan/miR-124 or miR-CTRL particles. Upper quadrants represent MHC-II-positive cells.

Three days after C3 spinal cord hemisection and intraperitoneal injection of chitosan formulated siRNA-Cy3 particles, small clusters of Cy3/ED-1 positive activated macrophages were found within 300-500 μm rostral and caudal to the injury site (Figure 5, *J-L*). The Cy3 signal in these blood-born macrophages appeared both as granular and diffuse staining (Figure 5, *J*).

Effects of miR-124 chitosan particles on macrophage/microglia reaction

Microinjection of 1 μL chitosan formulated miR-CTRL particles into intact cervical C3 spinal cord of adult rats induced activation of ED-1 positive macrophages and microglial cells along the injury canal left after withdrawal of the 70 μm thick tip of the glass micropipette (Figure 6, *A, C*). In contrast, injection of particles with miR-124 reduced the number of ED-1 labelled cells by 80% (*P*<0.001; Figure 6, *B, C*).

In the experiments with spinal cord injury, the rats underwent cervical C3 hemisection and chitosan formulated miR-CTRL particles were injected 1 mm rostral and caudal to the injury site. The reaction of ED-1 positive macrophages and microglial cells was measured in the trauma zone. Injections of miR-124 containing particles reduced the number of ED-1 positive cells by 60% (*P*<0.001; Figure 7).

However, when miR-124 particles were introduced into the spinal cord cavity within a small piece of Spongostan®, no reduction in macrophage and microglia activity was found (data not shown).

Discussion

Active macrophages/microglia play a central role in traumatic SCIs as well as in the progression of certain neurodegenerative diseases, including Parkinson's disease,[35] multiple sclerosis (MS),[36] and Alzheimer's disease.[37] As such, reducing CNS inflammation presents a promising strategy for treatment of multiple neurodegenerative disorders. By administering miR-124/chitosan polyplex particles in rat models of spinal cord inflammation, we successfully altered the inflammatory response by affecting the transcriptome of local macrophages/microglia.

We describe formulations of non-toxic chitosan particles for the effective delivery of miR-124. It has been previously reported that uptake of 150–300 nm chitosan-DNA particles is cell-type dependent.[38] Our studies have demonstrated that similar size chitosan particles can provide delivery of small interfering RNA (siRNA) to different cell types and the efficacy of uptake is also cell-type dependent and can vary based on the MW and degree of deacetylation.[27,31] The present results show that ~160 nm siRNA-Cy3/chitosan particles have been taken up by nearly all cultured macrophages and the functional efficiency of the ~220 nm miR-124/chitosan particles (based on the number of MHC-II positive cells) was about 50%. Chitosan is known to be an effective agent for siRNA complexation, and capable of delivery to various types of macrophages.[26,31,39] Although the chitosan system does not specifically target any particular cell type, they are shown here to be internalized solely by microglia/macrophages *in vivo*. Transfection of cationic polyplexes mediated by charge interactions between the positive surface charge of the particle and the negatively charged cell membrane. It is believed that chitosan particles transfect cells via endocytic/phagocytic activity, and subsequently escape the endosome/lysosome either by the "proton sponge effect", or by the degradation products of the polymer increasing the osmolality and thereby rupturing the endosome.[38,40] The innate specificity for targeting macrophages/microglia with the miR-124 mimic rather than astrocytes is important in that the regulation of STAT3 in astrocytes can prevent the organization of the astrocytic penumbra of the glial scar, which can lead to an increased inflammation response.[41–43]

Our results support and complement a previous study in mice showing that miR-124 transfection reduces MHC-II, TNF-α and ROS production in bone marrow derived macrophages.[20] However, as previous studies have alleged that certain MW of chitosan have an effect on the polarization state of macrophages,[44,45] it is important to note that our results are specifically dependent on the RNA sequence in complex with chitosan, and not due to the chitosan itself.

While microinjections present a convenient model of CNS inflammation simply due to the physical disruption of the blood brain barrier (BBB) by the needle cavity, the clinical application
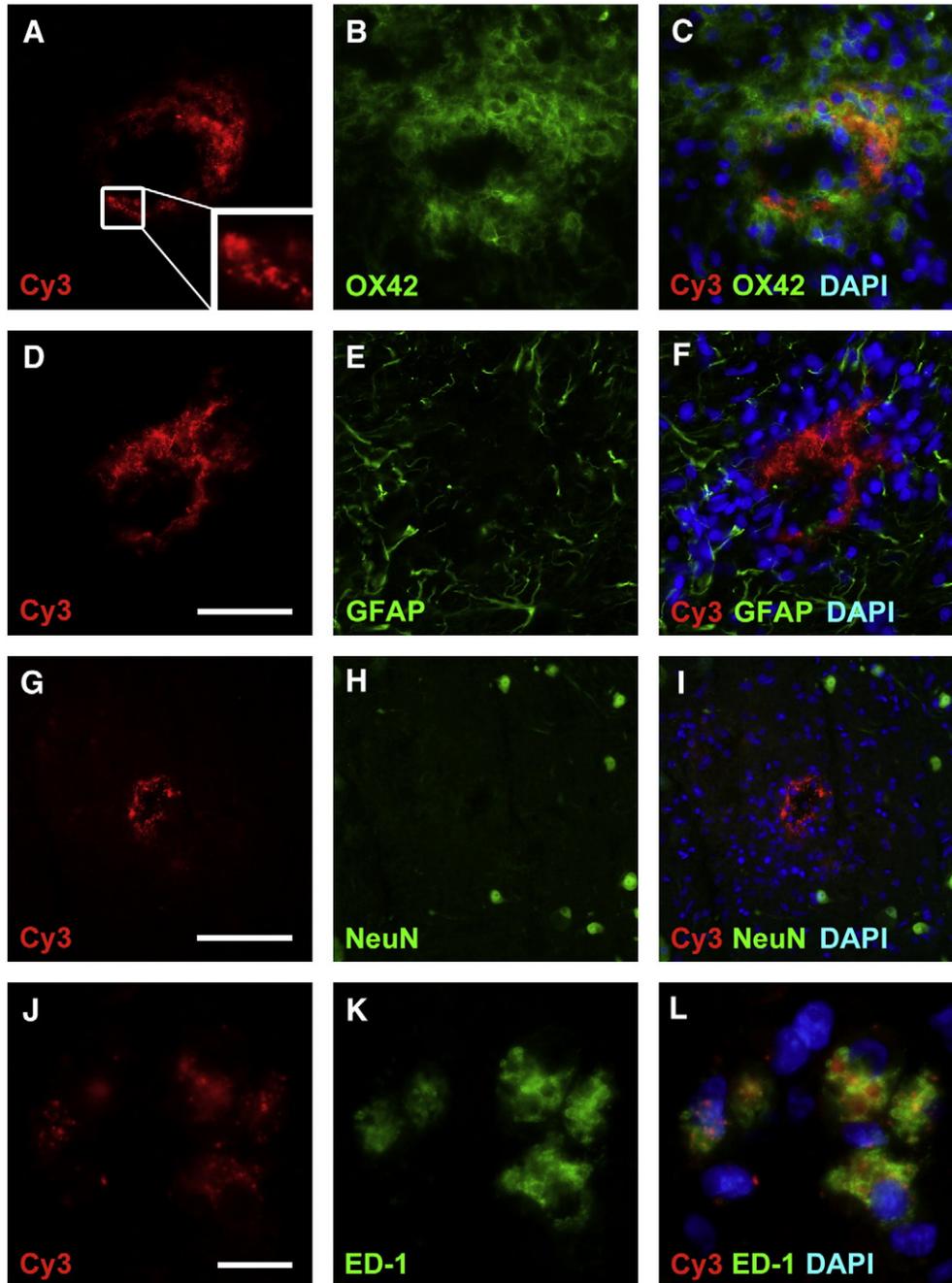
Figure 5. Horizontal spinal cord sections of C3 segments showing siRNA-Cy3/chitosan particles (Cy3) 3 days after injection into normal spinal cord (**A–I**) and after intraperitoneal injection in animals with spinal cord injury (**J–L**). Sections were immunostained for OX42 (CD11b, macrophages and microglia), GFAP (astrocytes), NeuN (neurons) and ED-1 (activated macrophages/microglia). Cell nuclei were stained using DAPI. Boxed area in (**A**) demonstrates details of injection site with small bright round particles and diffuse staining. Note association of Cy3 labelled particles with OX42 and ED-1 positive cells. Scale bar, 50 μm (**A–F**), 100 μm (**G–I**) and 20 μm (**J–L**).

of such an invasive technique is minimal. Disruption of the BBB during traumatic injury, Alzheimers disease,[46] MS,[47] and Parkinsons disease [48] leads to a host of complications for CNS repair, but can also provide an avenue for infiltration of therapeutics from the blood stream. By loading macrophages with particles containing catalase, and injecting them intraper-

itoneally into an induced mouse model of Parkinson's disease, particle loaded macrophages have been shown to localize in the affected midbrain and protect neurons by reducing ROS species.[49] Chitosan particles have previously been found to be transported with recruited macrophages to sites of inflammation in a mouse models of rheumatoid arthritis,[31] radiation induced
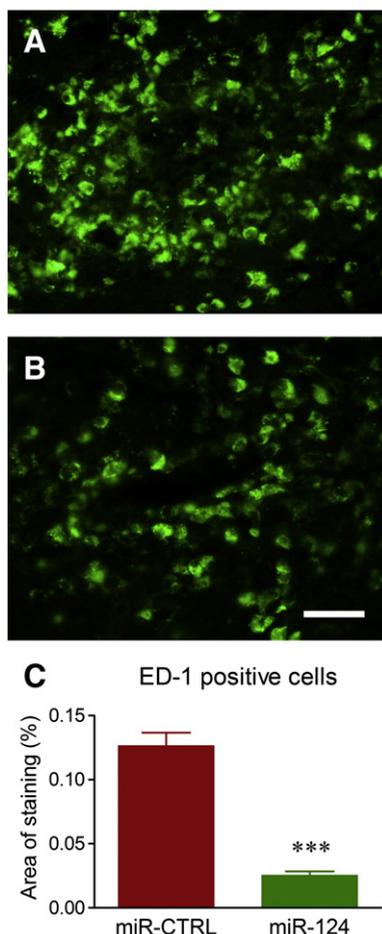
Figure 6. Horizontal sections of C3 spinal segments with ED-1 positive macrophages and microglia 3 days after injection of miR-CTRL (**A**) and miR-124 (**B**) chitosan particles into normal spinal cord. Histogram showing the relative tissue area occupied by ED-1 positive macrophages and microglial cells (**C**). Error bars show S.E.M. $P<0.001$ is indicated by ***. Scale bar, 50 µm.

The miR-124 particle treatment was effective in reducing local ED-1 positive cells in an acute *in vivo* SCI model. Long-term experiments are needed to study the effect miR-124/chitosan particles may have on the secondary tissue disruption associated with SCI. It is certainly conceivable from the evidence presented that the marked reduction of ED-1 expressing macrophages/microglia in miR-124 treated SCI's correlate with a reduction in inflammatory secretome expression.

Polarization of microglia/macrophages to the activated M1 phenotype is linked to the sustained inflammatory conditions of neurodegenerative diseases; the alternatively activated M2 phenotype performs the opposite function and enhances neuroprotection and regeneration in SCI.[55] Therefore the strategy employed herein, to reduce neurotoxic agents in the CNS by delivering miR-124 to induce macrophage quiescence, has the potential to be enhanced further by exploring the possibility of promoting M2 polarization over that of M1. As we have successfully shown delivery of miRNA/particles to M1 activated macrophages/microglia and the subsequent reduction of negative effects thereof, a similar strategy could be employed to deliver a miRNA responsible for promoting the transition of M1 to M2 polarization or by delivering an anti-miR to reduce the effect of an M1 specific miRNAs. An anti-miR towards miR-155 could also be a viable option for delivery to SCIs as the miRNA has been shown to promote M1 polarization in human macrophages while its inhibition blunts the expression of pro-inflammatory cytokines in a MS model.[56] It has recently been shown that miRNA let-7c promotes M2 polarization by regulating C/EBP-δ in mouse bone marrow derived macrophages and is conversely associated with M1 polarization upon silencing using anti-miRs.[57]

Taken together, our data presents the chitosan polyplex system as a promising method for the delivery of miRNA to specifically modulate macrophage/microglia activation, and subsequently reduce neuroinflammation *in vivo*.

fibrosis,[29,39] kidney fibrosis,[50] and periodontal lesions.[51] To evaluate if the same mode of delivery is available for use in future CNS inflammation studies, we surgically performed SCIs, followed by intraperitoneal injection of chitosan particles to assess the recruitment of the particle loaded macrophages to the injury site. The migration of peritoneal macrophages to the spinal cord lesion was validated by the detection of internalized chitosan/siRNA-Cy3 particles. It remains to be seen if miR-124 can have the same effect on macrophage activation in SCIs if delivered to the peritoneum, as these cells may not be as motile when quiescent.[52,53] Additionally, motility may directly be affected by miR-124 targeting STAT3, as this signaling pathway has been shown to regulate cell movement in keratinocytes, leukocytes, and epidermal cells.[54] Regardless of the cargo, this delivery strategy presents a promising, minimally invasive means to address CNS inflammation in future studies and may also provide a method of quantifying and studying the effects and the resident vs. migratory macrophage population in such conditions.

Author Contributions

The manuscript was written by AML with contributions from LeN, and JK. *Ex vivo* experiments were performed by AML, and *in vivo* studies by MKK, LeN and LuN. PJK, LeN, MW and JK supervised the project. All authors have given approval to the final version of the manuscript.

Appendix A. Supplementary data

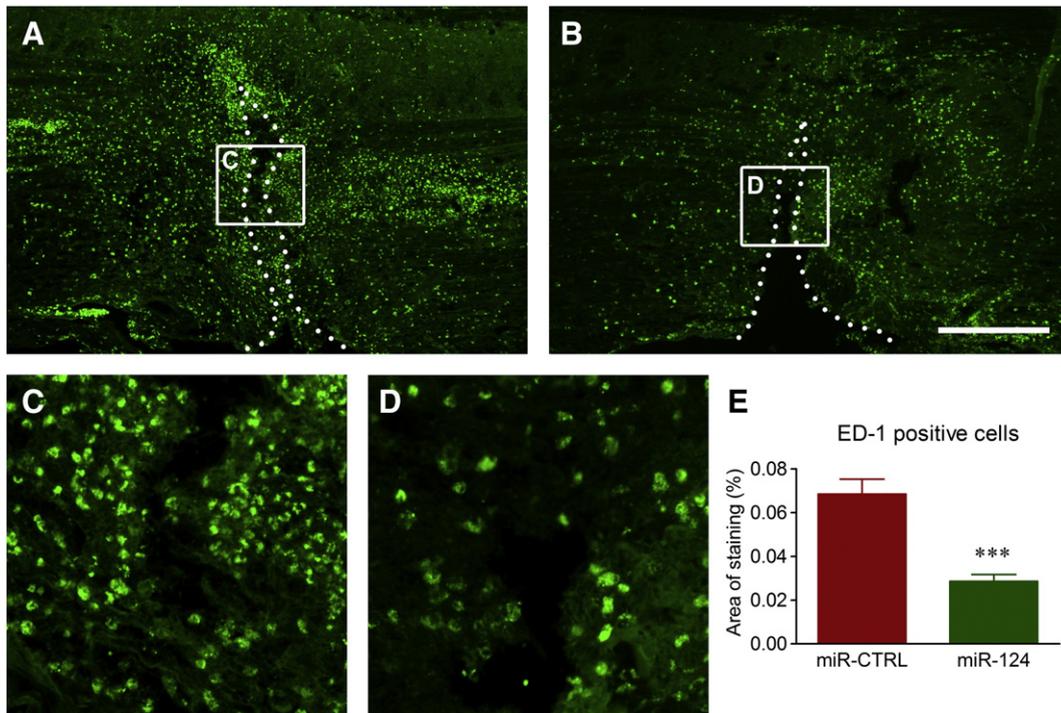Supplementary data to this article can be found online at http://dx.doi.org/10.1016/j.nano.2015.10.011.

Figure 7. Horizontal spinal cord sections of C3-C4 segments (**A, B**) immunostained for ED-1 positive macrophages and microglial cells 3 days after spinal cord hemisection followed by intraspinal injection of miR-CTRL (**A**) and miR-124 (**B**) chitosan particles. Dotted lines indicate primary trauma zone. Boxed areas in (**A**) and (**B**) are enlarged in (**C**) and (**D**), respectively. Note significant reduction of ED-1 immunostaining in (**B**). Histogram showing the relative tissue area occupied by ED-1 positive macrophages and microglial cells (**E**). Error bars show S.E.M. $P<0.001$ is indicated by ***. Scale bar, 500 μm.

References

1. Center NSCIS, 2013. Annual Statistical Report for the Spinal Cord Model Injury Systems - Complete Public Version, University of Alabama at Birmingham, Alabama, The National Spinal Cord Injury Center, Birmingham, Alabama

2. Silver J, Miller JH. Regeneration beyond the glial scar. *Nat Rev Neurosci* 2004;**5**:146-56.

3. Kierdorf K, Erny D, Goldmann T, Sander V, Schulz C, Perdiguero EG, et al. Microglia emerge from erythromyeloid precursors via Pu.1- and Irf8-dependent pathways. *Nat Neurosci* 2013;**16**:273-80.

4. Ransohoff RM, Cardona AE. The myeloid cells of the central nervous system parenchyma. *Nature* 2010;**468**:253-62.

5. Larrick JW, Wright SC. Cytotoxic mechanism of tumor necrosis factor-alpha. *FASEB J* 1990;**4**:3215-23.

6. Kaushal V, Koeberle PD, Wang Y, Schlichter LC. The Ca2+-activated K+ channel KCNN4/KCa3.1 contributes to microglia activation and nitric oxide-dependent neurodegeneration. *J Neurosci* 2007;**27**:234-44.

7. Bao F, Bailey CS, Gurr KR, Bailey SI, Rosas-Arellano MP, Dekaban GA, et al. Increased oxidative activity in human blood neutrophils and monocytes after spinal cord injury. *Exp Neurol* 2009;**215**:308-16.

8. Colton CA, Gilbert DL. Production of superoxide anions by a CNS macrophage, the microglia. *FEBS Lett* 1987;**223**:284-8.

9. Qi L, Jacob A, Wang P, Wu R. Peroxisome proliferator activated receptor-gamma and traumatic brain injury. *Int J Clin Exp Med* 2010;**3**:283-92.

10. Yi JH, Park SW, Brooks N, Lang BT, Vemuganti R. PPARgamma agonist rosiglitazone is neuroprotective after traumatic brain injury via anti-inflammatory and anti-oxidative mechanisms. *Brain Res* 2008;**1244**:164-72.

11. Haber M, Abdel Baki SG, Grin'kina NM, Irizarry R, Ershova A, Orsi S, et al. Minocycline plus N-acetylcysteine synergize to modulate inflammation and prevent cognitive and memory deficits in a rat model of mild traumatic brain injury. *Exp Neurol* 2013;**249**:169-77.

12. Noble LJ, Donovan F, Igarashi T, Goussev S, Werb Z. Matrix metalloproteinases limit functional recovery after spinal cord injury by modulation of early vascular events. *J Neurosci* 2002;**22**:7526-35.

13. Gao HM, Liu B, Zhang W, Hong JS. Critical role of microglial NADPH oxidase-derived free radicals in the in vitro MPTP model of Parkinson's disease. *FASEB J* 2003;**17**:1954-6.

14. Huh Y, Jung JW, Park C, Ryu JR, Shin CY, Kim WK, et al. Microglial activation and tyrosine hydroxylase immunoreactivity in the substantia nigral region following transient focal ischemia in rats. *Neurosci Lett* 2003;**349**:63-7.

15. McGeer PL, Schwab C, Parent A, Doudet D. Presence of reactive microglia in monkey substantia nigra years after 1-methyl-4-phenyl-1,2,3,6-tetrahydropyridine administration. *Ann Neurol* 2003;**54**:599-604.

16. Davis MJ, Tsang TM, Qiu Y, Dayrit JK, Freij JB, Huffnagle GB, et al. Macrophage M1/M2 polarization dynamically adapts to changes in cytokine microenvironments in *Cryptococcus neoformans* infection. *MBio* 2013;**4**:e00264-13.

17. Bartel DP. MicroRNA target recognition and regulatory functions. *Cell* 2009;**136**:215-33.

18. Mishima T, Mizuguchi Y, Kawahigashi Y, Takizawa T, Takizawa T. RT-PCR-based analysis of microRNA (miR-1 and -124) expression in mouse CNS. *Brain Res* 2007;**1131**:37-43.

19. Makeyev EV, Zhang J, Carrasco MA, Maniatis T. The MicroRNA miR-124 promotes neuronal differentiation by triggering brain-specific alternative pre-mRNA splicing. *Mol Cell* 2007;**27**:435-48.

20. Ponomarev ED, Veremeyko T, Barteneva N, Krichevsky AM, Weiner HL. MicroRNA-124 promotes microglia quiescence and suppresses EAE by deactivating macrophages via the C/EBP-alpha-PU.1 pathway. *Nat Med* 2011;**17**:64-70.

21. Cai DH, Wang D, Keefer J, Yeamans C, Hensley K, Friedman AD. C/EBP alpha:AP-1 leucine zipper heterodimers bind novel DNA elements, activate the PU.1 promoter and direct monocyte lineage commitment more potently than C/EBP alpha homodimers or AP-1. *Oncogene* 2008;**27**:2772-9.

22. Feng R, Desbordes SC, Xie H, Tillo ES, Pixley F, Stanley ER, et al. PU.1 and C/EBPalpha/beta convert fibroblasts into macrophage-like cells. *Proc Natl Acad Sci U S A* 2008;**105**:6057-62.

23. Walton M, Saura J, Young D, MacGibbon G, Hansen W, Lawlor P, et al. CCAAT-enhancer binding protein alpha is expressed in activated microglial cells after brain injury. *Brain Res Mol Brain Res* 1998;**61**:11-22.

24. Ponomarev ED, Veremeyko T, Weiner HL. MicroRNAs are universal regulators of differentiation, activation, and polarization of microglia and macrophages in normal and diseased CNS. *Glia* 2013;**61**:91-103.

25. Sun Y, Li Q, Gui H, Xu DP, Yang YL, Su DF, et al. MicroRNA-124 mediates the cholinergic anti-inflammatory action through inhibiting the production of pro-inflammatory cytokines. *Cell Res* 2013;**23**:1270-83.

26. Howard KA, Rahbek UL, Liu X, Damgaard CK, Glud SZ, Andersen MO, et al. RNA interference in vitro and in vivo using a novel chitosan/siRNA nanoparticle system. *Mol Ther* 2006;**14**:476-84.

27. Liu X, Howard KA, Dong M, Andersen MO, Rahbek UL, Johnsen MG, et al. The influence of polymeric properties on chitosan/siRNA nanoparticle formulation and gene silencing. *Biomaterials* 2007;**28**:1280-8.

28. Ballarin-Gonzalez B, Dagnaes-Hansen F, Fenton RA, Gao S, Hein S, Dong M, et al. Protection and systemic translocation of siRNA following oral administration of chitosan/siRNA nanoparticles. *Mol Ther Nucleic Acids* 2013;**2**:e76.

29. Nawroth I, Alsner J, Deleuran BW, Dagnaes-Hansen F, Yang C, Horsman MR, et al. Peritoneal macrophages mediated delivery of chitosan/siRNA nanoparticle to the lesion site in a murine radiation-induced fibrosis model. *Acta Oncol* 2013;**52**:1730-8.

30. Mittnacht U, Hartmann H, Hein S, Oliveira H, Dong M, Pego AP, et al. Chitosan/siRNA nanoparticles biofunctionalize nerve implants and enable neurite outgrowth. *Nano Lett* 2010;**10**:3933-9.

31. Howard KA, Paludan SR, Behlke MA, Besenbacher F, Deleuran B, Kjems J. Chitosan/siRNA nanoparticle-mediated TNF-alpha knockdown in peritoneal macrophages for anti-inflammatory treatment in a murine arthritis model. *Mol Ther* 2009;**17**:162-8.

32. Andersen MO, Howard KA, Paludan SR, Besenbacher F, Kjems J. Delivery of siRNA from lyophilized polymeric surfaces. *Biomaterials* 2008;**29**:506-12.

33. Frank MG, Wieseler-Frank JL, Watkins LR, Maier SF. Rapid isolation of highly enriched and quiescent microglia from adult rat hippocampus: immunophenotypic and functional characteristics. *J Neurosci Methods* 2006;**151**:121-30.

34. Havenith CE, Askew D, Walker WS. Mouse resident microglia: isolation and characterization of immunoregulatory properties with naive CD4+ and CD8+ T-cells. *Glia* 1998;**22**:348-59.

35. Kurkowska-Jastrzebska I, Wronska A, Kohutnicka M, Czlonkowski A, Czlonkowska A. MHC class II positive microglia and lymphocytic infiltration are present in the substantia nigra and striatum in mouse model of Parkinson's disease. *Acta Neurobiol Exp (Wars)* 1999;**59**:1-8.

36. Howell OW, Rundle JL, Garg A, Komada M, Brophy PJ, Reynolds R. Activated microglia mediate axoglial disruption that contributes to axonal injury in multiple sclerosis. *J Neuropathol Exp Neurol* 2010;**69**:1017-33.

37. Akiyama H. Alzheimer's disease and the immune system response. *Nihon Rinsho* 1994;**52**:2990-4.

38. Mao HQ, Roy K, Troung-Le VL, Janes KA, Lin KY, Wang Y, et al. Chitosan-DNA nanoparticles as gene carriers: synthesis, characterization and transfection efficiency. *J Control Release* 2001;**70**:399-421.

39. Nawroth I, Alsner J, Behlke MA, Besenbacher F, Overgaard J, Howard KA, et al. Intraperitoneal administration of chitosan/DsiRNA nanoparticles targeting TNFalpha prevents radiation-induced fibrosis. *Radiother Oncol* 2010;**97**:143-8.

40. Behr JP. The proton sponge: A trick to enter cells the viruses did not exploit. *CHIMIA Int J Chem* 1997;**51**:34-6.

41. Okada S, Nakamura M, Katoh H, Miyao T, Shimazaki T, Ishii K, et al. Conditional ablation of Stat3 or Socs3 discloses a dual role for reactive astrocytes after spinal cord injury. *Nat Med* 2006;**12**:829-34.

42. Herrmann JE, Imura T, Song B, Qi J, Ao Y, Nguyen TK, et al. STAT3 is a critical regulator of astrogliosis and scar formation after spinal cord injury. *J Neurosci* 2008;**28**:7231-43.

43. Wanner IB, Anderson MA, Song B, Levine J, Fernandez A, Gray-Thompson Z, et al. Glial scar borders are formed by newly proliferated, elongated astrocytes that interact to corral inflammatory and fibrotic cells via STAT3-dependent mechanisms after spinal cord injury. *J Neurosci* 2013;**33**:12870-86.

44. Chung MJ, Park JK, Park YI. Anti-inflammatory effects of low-molecular weight chitosan oligosaccharides in IgE-antigen complex-stimulated RBL-2H3 cells and asthma model mice. *Int Immunopharmacol* 2012;**12**:453-9.

45. Yoon HJ, Moon ME, Park HS, Im SY, Kim YH. Chitosan oligosaccharide (COS) inhibits LPS-induced inflammatory effects in RAW 264.7 macrophage cells. *Biochem Biophys Res Commun* 2007;**358**:954-9.

46. Kook SY, Seok Hong H, Moon M, Mook-Jung I. Disruption of blood-brain barrier in Alzheimer disease pathogenesis. *Tissue Barriers* 2013;**1**:e23993.

47. Minagar A, Alexander JS. Blood-brain barrier disruption in multiple sclerosis. *Mult Scler* 2003;**9**:540-9.

48. Lee H, Pienaar IS. Disruption of the blood-brain barrier in Parkinson's disease: curse or route to a cure? *Front Biosci (Landmark Ed)* 2014;**19**:272-80.

49. Klyachko NL, Haney MJ, Zhao Y, Manickam DS, Mahajan V, Suresh P, et al. Macrophages offer a paradigm switch for CNS delivery of therapeutic proteins. *Nanomedicine (Lond)* 2014;**9**:1403-22.

50. Yang C, Nilsson L, Cheema MU, Wang Y, Frokiaer J, Gao S, et al. Chitosan/siRNA nanoparticles targeting cyclooxygenase type 2 attenuate unilateral ureteral obstruction-induced kidney injury in mice. *Theranostics* 2015;**5**:110-23.

51. Ma Z, Dagnaes-Hansen F, Lovschall H, Song W, Nielsen GK, Yang C, et al. Macrophage-mediated nanoparticle delivery to the periodontal lesions in established murine model via Pg-LPS induction. *J Oral Pathol Med* 2015;**44**:538-42.

52. Enomoto A, Murakami H, Asai N, Morone N, Watanabe T, Kawai K, et al. Akt/PKB regulates actin organization and cell motility via Girdin/APE. *Dev Cell* 2005;**9**:389-402.

53. Traynor D, Kay RR. Possible roles of the endocytic cycle in cell motility. *J Cell Sci* 2007;**120**:2318-27.

54. Hirano T, Ishihara K, Hibi M. Roles of STAT3 in mediating the cell growth, differentiation and survival signals relayed through the IL-6 family of cytokine receptors. *Oncogene* 2000;**19**:2548-56.

55. Kigerl KA, Gensel JC, Ankeny DP, Alexander JK, Donnelly DJ, Popovich PG. Identification of two distinct macrophage subsets with divergent effects causing either neurotoxicity or regeneration in the injured mouse spinal cord. *J Neurosci* 2009;**29**:13435-44.

56. Moore CS, Rao VTS, Durafourt BA, Bedell BJ, Ludwin SK, Bar-Or A, et al. miR-155 as a multiple sclerosis–relevant regulator of myeloid cell polarization. *Ann Neurol* 2013;**74**:709-20.

57. Banerjee S, Xie N, Cui H, Tan Z, Yang S, Icyuz M, et al. MicroRNA let-7c regulates macrophage polarization. *J Immunol* 2013;**190**:6542-9.